

NASA-CR-199355

NA55-32861
IN-45-CR
65489
p.32

COMPOSITION, CHEMISTRY, AND CLIMATE OF THE ATMOSPHERE

▼
Edited by

Hanwant B. Singh



VAN NOSTRAND REINHOLD
I(T)P™ A Division of International Thomson Publishing Inc.

New York • Albany • Bonn • Boston • Detroit • London • Madrid • Melbourne
Mexico City • Paris • San Francisco • Singapore • Tokyo • Toronto

(NASA-CR-199355) COMPOSITION,
CHEMISTRY, AND CLIMATE OF THE
ATMOSPHERE. 2: MEAN PROPERTIES OF
THE ATMOSPHERE (Van Nostrand
Reinhold) 32 p

N96-16030

Unclass

G3/45 0065489

2

Mean properties of the atmosphere

David A. Salstein

- 2.1. INTRODUCTION
 - 2.2. GOVERNING EQUATIONS
 - 2.3. TIME AND SPACE SCALES OF ATMOSPHERIC PROPERTIES
 - 2.4. MEAN METEOROLOGICAL QUANTITIES
 - 2.4.1. The Climate Diagnostics Database
 - 2.4.2. Temperature Structure
 - 2.4.3. Wind Structure
 - 2.4.4. Humidity Structure
 - 2.4.5. Meridional Eddy Transport of Heat and Momentum
 - 2.5. HEATING OF THE ATMOSPHERE
 - 2.6. BOUNDARY LAYER OVERVIEW
 - 2.7. MAJOR EXCHANGES IN THE ATMOSPHERE
- Acknowledgments
References

2.1. INTRODUCTION

The atmosphere can be defined as the relatively thin gaseous envelope surrounding the entire planet Earth. It possesses a number of properties related to its physical state and chemical composition, and it undergoes a variety of internal processes and external interactions that can either maintain or alter these properties. Whereas descriptions of the atmosphere's chemical properties form much of the remaining chapters of this book, the present chapter will highlight the atmosphere's physical and dynamical properties, including its temperature, pressure, and motions. Internal energy is contained in the molecular motions of the atmosphere's gases, and these define its temperature structure. In contrast, the larger-scale motions comprise the winds, the global organization of which is often referred to as the general circulation. The framework of the dynamical and thermodynamical laws, including the three principles of conservation of mass, momentum, and energy, are fundamental in describing both the internal processes of the atmosphere and its external interactions. The atmosphere is not

a closed system, because it exchanges all three of these internally conservative quantities across the atmosphere's boundary below and receives input from regions outside it. Thus surface fluxes of moisture, momentum, and heat occur to and from the underlying ocean and land. The atmosphere exchanges very little mass and momentum with space, though it absorbs directly a portion of the solar radiational energy received from above.

The total dry mass of the atmosphere, calculated as an annual mean, is estimated to be 5.13×10^{18} kg (Trenberth and Guillemot, 1994). The atmosphere exists in a space that has as its lower boundary the land surface, whose irregular topography results in a varying surface geopotential, as well as the relatively equipotential ocean surface. Thus the local atmospheric surface pressure, and hence the quantity of its mass above an area, varies considerably from one geographical area to another. The extent of topographical features is such that a difference of nearly 3% exists between the mean surface pressure at sea level, near 1013 mbar, and its global mean calculated over both land and ocean, the value of which is estimated to be 984 mbar. However, locally, over the highest mountains, which reach an altitude of over 8000 m, the pressure may be as low as 300 mbar, less than one-third of that at sea level. A representation of the surface pressure of the atmosphere, smoothed to eliminate the smallest features, is given in Figure 2.1. Clear from the figure is the dependence of surface pressure on the orography. In addition, the mean surface pressure depends somewhat on the characteristics of predominant air masses, and hence on temperature as well

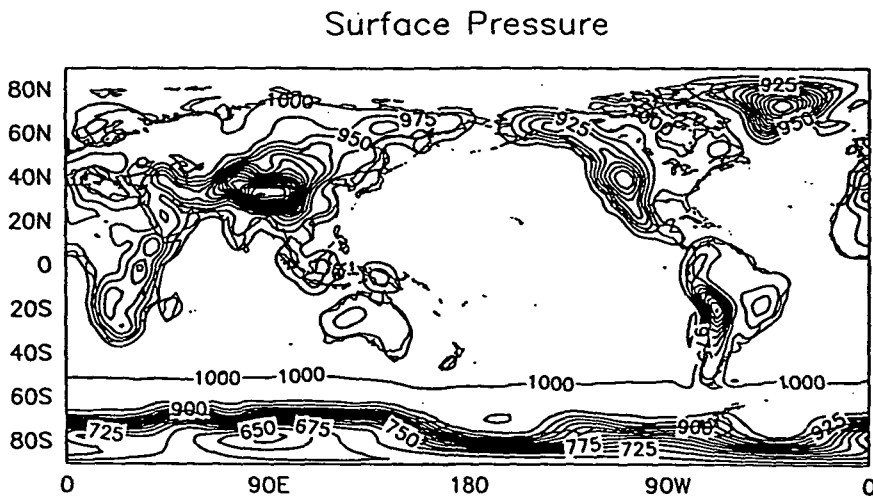


FIGURE 2.1. Mean surface pressure of the atmosphere, taken from the US National Meteorological Center analyses. The period 1980–1985 was chosen as the period on which to base the figure. Units are millibars, where 10^2 Pa = 1 mbar.

as land surface height. For example, areas at sea level north of 50° S have pressures exceeding 1000 mbar, whereas those south of 50° S are generally under 1000 mbar.

The temperature structure of the atmosphere is such that it is often considered to be stratified in the vertical into several layers. The lowest region, the troposphere, where temperature decreases everywhere with altitude (and hence with decreasing pressure), extends to a level of about 10 km, near the 1000 mbar level, although its upper boundary, termed the tropopause, varies with latitude and season. The stability of the atmosphere is a measure of the potential of air to remain static vertically at a constant pressure level and thus resist overturning. This static stability varies considerably in the troposphere, and when it is negative, convection often leads to the production of clouds. At the bottom of the troposphere is the relatively thin boundary layer, where the atmosphere interacts most strongly with the surface below. Above the troposphere is the stratosphere, a very stable region, where temperature increases with altitude. The lower

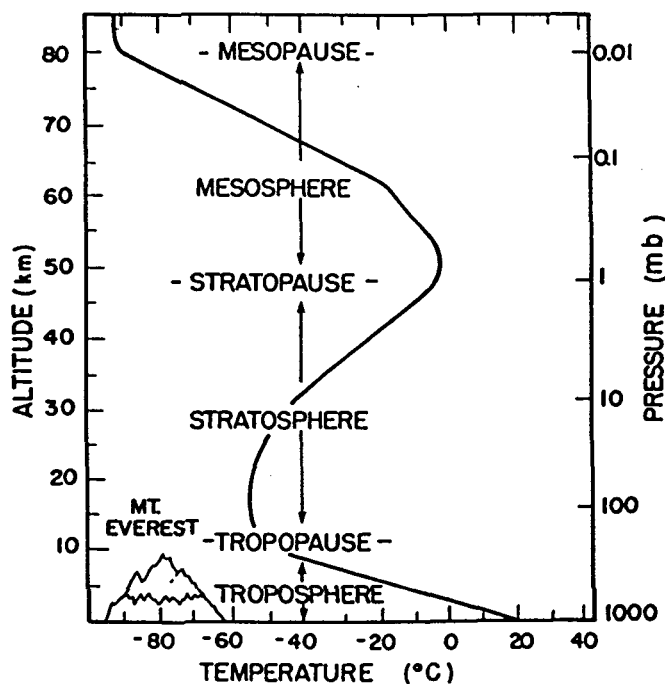


FIGURE 2.2. Schematic picture of the vertical temperature structure of the atmosphere. The commonly defined regions of the atmosphere and their upper limits are noted. The atmospheric pressures approximating the heights are given as well. (Adapted from US Standard Atmosphere, 1976.)

TABLE 2.1 Bulk Mean Mixing Ratios of Major and Minor Constituents of the Global Atmosphere

Gas	Average Mixing Ratio in parts per million (% by volume) ^a	Remarks
N ₂	780,840 (78.1%)	Biological
O ₂	209,460 (20.9%)	Biological
Ar	9340 (0.9%)	Inert
CO ₂	350 (0.03%)	Variable, secular increase
Ne	18	Inert
He	5.2	Inert
CH ₄	1.7	Biogenic and anthropogenic
H ₂	0.6	Biogenic and anthropogenic
N ₂ O	0.31	Biogenic and anthropogenic
CO	0.03–0.2	Anthropogenic and chemical
O ₃	0.01–0.15	Photochemical
Non-methane hydrocarbons	0.005–0.02	Biogenic and anthropogenic
Halocarbons	0.002	75% man-made; long-lived
Sulfur species	0.0005–0.001	Biogenic and anthropogenic
Nitrogen species (NO _y) ^b	0.0001–0.001	Anthropogenic

^aOn a dry basis. Water vapor is a highly variable physicochemical component of the atmosphere.

^bHigh concentrations of O₃ (5–10 ppm) and NO_y (0.02 ppm) are present in the stratosphere.

stratosphere is hence a minimum level of temperature, and the temperature there is lowest in the tropics. In the stratosphere, interactions with solar radiation have special importance, because molecules there, especially ozone (O₃), absorb the strong ultraviolet solar radiation, shielding the Earth's surface below from its effects. Above the stratosphere are the mesosphere (starting near 47 km, or 1 mbar) and the thermosphere (from about 85 km, or somewhat less than 0.01 mbar). These two high regions have respectively decreasing and increasing vertical lapse rates of temperature. In even higher regions, matter exists in an ionized state and becomes particularly reactive with the solar radiation. A plot of average temperature in these regions is given in Figure 2.2.

The major constituents of air are molecular nitrogen, oxygen, and, to a smaller extent, argon, comprising 99.9% by volume. The remaining portion includes carbon dioxide, whose concentration has been observed to increase significantly in historic times owing to anthropogenic causes. Trace gases include ozone, methane (CH₄), oxides of nitrogen, carbon monoxide (CO), and halocarbons. The proportions of the major dry atmospheric gases are summarized in Table 2.1. Water vapor, a particularly variable atmospheric constituent, resides almost entirely in the lower and middle troposphere; its changing structure will be examined below.

2.2. GOVERNING EQUATIONS

To put the distribution and fluctuations of the mean quantities of the atmosphere in perspective, we rely on a framework based on the conservation principles of physics. In this way, expression of physical laws regarding the atmosphere reveals which atmospheric quantities are important to monitor. Also, they form the basis for the set of equations governing the state and dynamics of the atmosphere, which, together with appropriate boundary and initial conditions, is typically utilized for weather forecasting. These physical principles include the conservation of mass, momentum, and energy.

Conservation of mass is expressible in the atmosphere as the so-called continuity equation, namely, a local change in density, $\partial\rho/\partial t$, is related to the divergence of the (three-dimensional) advection of mass into the area by the vector wind v :

$$\partial\rho/\partial t = -\nabla \cdot \rho v \quad (2.1)$$

This equation leads to the condition in the general circulation that vertical and horizontal flow of the air balance over periods longer than about 1 month, because changes in mass storage on these times scales are not significant. Also, individual constituents such as water vapor, to the extent that they are chemically non-reactive, obey similar conservation laws. In this regard, external sources and sinks of water vapor in the atmosphere, by evaporation and condensation, are solely responsible for changes in the overall quantities of water vapor. Assuming no large change in liquid water storage of clouds over much time, records of precipitation can substitute for condensation.

The principle of conservation of momentum is usually formulated by the atmospheric equations of motion, equivalent to an expression of Newton's second law. In this way, momentum can change locally by advection, and by external forces. When given in the framework of the Earth's rotating coordinate system, local changes in momentum per unit mass are expressible as

$$\partial v/\partial t = -v \cdot \nabla v - 2\Omega \times v - \nabla p/\rho + g + F \quad (2.2)$$

Here local changes in the three-dimensional velocity vector are accomplished in five ways: by advection of momentum; by the Coriolis force $-2\Omega \times v$ acting normal to the velocity vector; by a pressure gradient body force; by the force of gravity; and by a friction force which can be against the Earth's surface. In equation (2.2), v is the horizontal velocity vector, Ω is the Earth's angular velocity, p is the pressure, ρ is the density, and g and F are the acceleration due to gravity, and surface friction, respectively.

The conservation of energy is expressed as the first law of thermodynamics, in which the quantity of internal energy per unit air mass is written as

$$c_p dT/dt = Q + \alpha dp/dt \quad (2.3)$$

where c_p is the specific heat of air at constant pressure, Q is the net (diabatic) heating rate per unit mass, and α is the specific volume ($\alpha = 1/p$). Use of the equation of state of the atmosphere, the ideal gas law, as well as the concept of potential temperature, allows us to transform this equation to a somewhat more direct form

$$(T/\theta)d\theta/dt = Q \quad (2.4)$$

Here the potential temperature $\theta = T(p_{00}/p)^\kappa$, with $\kappa = 2/7$, is defined as the temperature that a parcel of air would attain if it were brought from its pressure p to a reference level p_{00} adiabatically. In standard meteorological practice this reference level is usually taken to be 1000 mbar.

The energy cycle of the atmosphere may be viewed as a convenient framework in which available potential energy is generated by heating processes, converted to kinetic form by means of baroclinic processes, and dissipated through frictional processes. Monitoring the large-scale aspects of the energy cycle, including measuring these various conversion terms, is a fundamental means for assessing the variability of the atmosphere, particularly on seasonal and longer time scales (Peixoto and Oort, 1974).

2.3. TIME AND SPACE SCALES OF ATMOSPHERIC PROPERTIES

To define the mean of a property in the atmosphere, we must consider both the time period and spatial extent over which to describe it. Because of the overwhelming solar forcing at the annual period, the year is often taken as the convenient unit over which to calculate mean properties. In addition to the mean value of a property over its annual period, the strength of the seasonal cycle, including the amplitudes of the annual and semi-annual components, can be important as well. Furthermore, the atmosphere has peaks of variability on much shorter scales, down, of course, to the daily period, a forcing also related to the solar heating variations. In between these time scales are variations on synoptic scales of about 1 week, related to the motion of weather systems, and intraseasonal scales of 1–2 months (Madden and Julian, 1971). However, when the strengths of atmospheric fluctuations on a whole range of scales are expressed as a kinetic energy spectrum, it is apparent that this spectrum has an especially strong, broad peak on the synoptic and shorter intraseasonal scales,

though of less magnitude than that on the annual scale (Peixoto and Oort, 1992).

On much longer, interannual periods, well-known features are the quasi-biennial oscillation (QBO), a reversal of the direction of the winds in the stratosphere occurring on roughly a 26 month cycle. Also prominent, with time scales of several years, is the so-called El Niño/Southern Oscillation (ENSO) phenomenon, a fluctuation of atmospheric mass across the Pacific Ocean, revealed by surface pressure anomalies, with an accompanying signature in the temperature of the ocean surface (Philander, 1989). During an ENSO event, wind and pressure fluctuations in patterns may occur within the year prior to and the 2 years following the warm peak in Pacific sea surface temperatures. The ENSO fluctuations are large enough to affect global measures of variability, including those of the general circulation. Because of the existence of these interannual variations, a measure of the mean state of the atmosphere should cover a multiyear period, approaching at least a decade.

Spatial scales are conveniently discussed first as the zonal averages of quantities over latitudinal bands. For quantities such as temperature, the distribution with latitude zones is considerable as well. In practice, the mean state of the atmosphere may be described on spatial scales that match the scales of common atmospheric forecasting and analysis models, which currently achieve a spectral resolution of order greater than 200 around the globe, where spatial-scale equivalence approaches 100 km at the equator; variations on finer scales are handled by parameterizations and are not explicitly part of the global analysis model.

Transports of quantities, namely advection by winds, are typically divided into those accomplished by mean motions and those due to smaller scale, eddy motions. Furthermore, the eddy terms have typically been divided into their transient and stationary components as follows. The transport by the wind, in, say, the meridional direction, of a quantity A over a period given by \overline{vA} (where the overbar denotes the time mean) can be decomposed into $\overline{vA} = \overline{v}\overline{A} + \overline{v'A'}$ (where primes indicate departures from the time mean). Likewise, the zonal average of the transport of a mean quantity $[\overline{vA}]$ (where brackets denote the zonal mean) is represented as $[\overline{vA}] = [\overline{v}][\overline{A}] \times [\overline{v^*A^*}]$ (where asterisks indicate departures from the zonal mean). These eddy terms, representing transient and stationary waves, respectively, may be thought of as independent means to transport meridionally the quantity A on a range of time and space scales.

2.4. MEAN METEOROLOGICAL QUANTITIES

As we have seen, fundamental meteorological variables in the atmosphere that appear in descriptions of the governing laws include the pressure, temperature, and wind. Also important are the moisture content of the atmosphere and the

proportions of other trace variables. This section will highlight the global distributions of many of these quantities. Also, the heating terms that drive the circulation are particularly important to understand and will be treated in the next section.

For forecast and analysis of weather features, specialized coordinate systems, particularly in the vertical, have been introduced into meteorology. Because the pressure decreases monotonically with height, observations are taken at given pressures, and because certain physical laws, such as the equation of continuity, are conveniently expressed in that system, analyses of many meteorological variables have often been given in pressure coordinates. The lowest such level for the vertical coordinate is usually taken at 1000 mbar. Additionally, though, forecast models of the atmosphere are often performed in other coordinate systems, such as a non-dimensional, terrain-following one. Other atmospheric descriptions of heating rates and studies of dynamics, including so-called diabatic circulations directly influenced by atmospheric heating, have been given in a vertical system based on potential temperature θ , defined above (Johnson, 1989); the θ coordinate can be used because it generally increases with increasing height monotonically. In this chapter, though, we will be confined to descriptions in pressure coordinates.

2.4.1 The Climate Diagnostics Database

Only a few data sets are available on which to base a global description of the mean atmospheric state. One such type is a special analysis of the atmosphere based on the large rawinsonde network comprised of around 1000 stations (Oort, 1983). A second type is derived from atmospheric analyses produced by the daily operational weather forecasting and data assimilation systems of the world's major weather centers. Though differences between operational analyses (Trenberth and Olson, 1988) and between rawinsonde and station analyses (Rosen et al., 1985) have been noted, we have chosen an archived set based on US National Meteorological Center (NMC) analyses (e.g., Kanamitsu, 1989). The vertical extent of these analyses encompasses the troposphere and lower stratosphere, and these regions are thus highlighted in our treatment of the mean quantities. This Climate Diagnostics Data Base (CDDB) has been organized into a set of monthly mean values of parameters and certain cross-products collected on a three-dimensional grid with $2.5^\circ \times 2.5^\circ$ resolution in latitude and longitude and on nine pressure levels in the vertical. From the monthly values, longer averages of one or many years can be formed and taken to represent the mean conditions of the atmosphere, and its variability can be represented as well (Rasmusson and Arkin, 1985).

Here we select one decade, 1980–1989, a period with reasonably reliable reporting, over which to describe atmospheric mean conditions, though it is not

as long as the 30 year period sometimes taken for climatological purposes. Although some changes that have taken place in the NMC operational system during the decade may produce inhomogeneities in the records, the use of the CDDB here for long-term mean fields is quite reasonable. Ultimately this inhomogeneity, more serious for studies of interannual fluctuations and trends, will be eliminated with the adoption of the Climate Data Assimilation System/Reanalysis System (Kalnay and Jenne, 1991). Such a system will produce analyses free from the heterogeneities associated with fluctuations in operational weather analysis procedures.

Besides the decade-long means for the annual period, we will display measures of both seasonal and interannual variability. The seasonal signals, which are often large compared with the long-term mean, are shown by the average of each calendar month for the 10 year period. Conversely, the interannual signal will constitute the mean of all 12 months within each calendar year; because it is typically small, it is given in anomaly form, i.e., the departure from the decade-long signal.

The CDDB fields are given for those levels of the atmosphere whose pressure is less than the mean surface pressure, i.e., above the physical topography. Those areas not plotted are blackened in the figures.

2.4.2 Temperature Structure

Because temperature is related to the heat balance, and hence energetics, of the atmosphere, and is important as well for reaction rates, it is a key parameter to diagnose. Of course, temperature varies with horizontal position as well as elevation. Aspects of its long-term mean, intraseasonal, and interannual variability are shown in Figures 2.3–2.6. In the first of these (Figure 2.3) the mean temperature averaged around a latitude band is given at the nine pressure levels, from 50 to 1000 mbar. Highest values of this zonal mean quantity, of course, occur in the tropics, having a tendency to peak near 10°N rather than at the equator; at the 1000 mbar level the temperature exceeds 295 K. The annual mean temperature structure is largely symmetric about the equator. Temperature generally decreases poleward, with differences between tropics and the highest latitude at the surface approaching 35 °C, and also upward, until near-stratospheric levels, where the meridional temperature gradient starts to reverse. In the tropical stratosphere, at 100 mbar, a minimum is found in the annual mean temperature values, reaching below 200 K; at this stratospheric level, temperature increases poleward by about 20 °C in both hemispheres.

A map of temperature at the lower tropospheric, 850 mbar level (Figure 2.4) expands the distribution of features into the longitudinal domain. The 850 mbar level was chosen because it is the first standard meteorological level above much of the topography and is a level at which a considerable quantity of heat energy

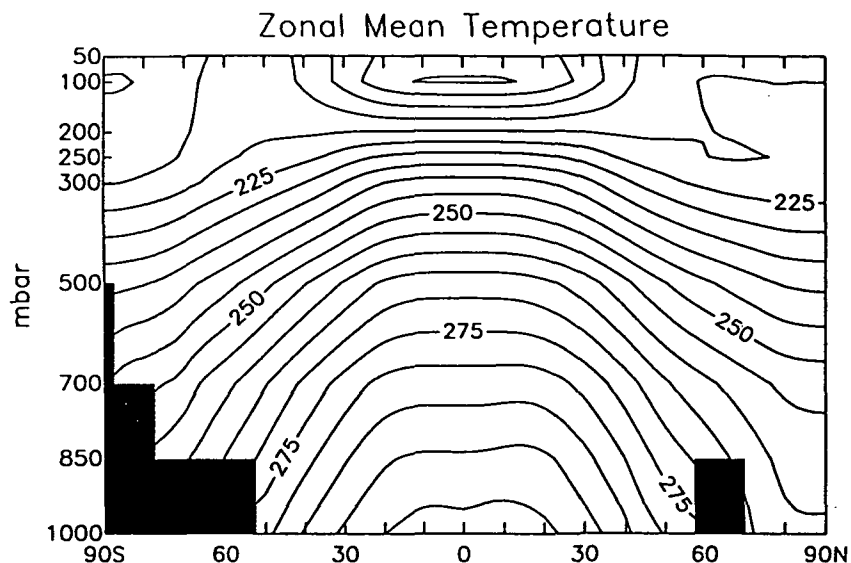


FIGURE 2.3. Zonal mean temperature for 1980–1989 between the 1000 and 50 mbar levels. Units are kelvins.

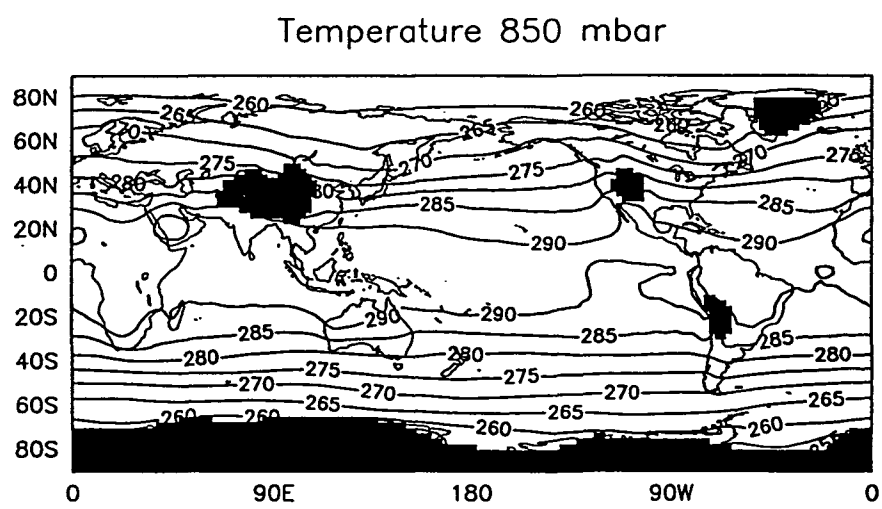


FIGURE 2.4. Mean temperature for 1980–1989 at the 850 mbar level. Units are kelvins.

is located as well as transported. It is clear that there is much zonal symmetry to the temperature structure of the atmosphere, particularly in the middle latitudes of the southern hemisphere. However, one can note asymmetries too, such as the troughs of lower temperatures dipping southward across North America and Eurasia (265–270 K contours), reflecting the colder, and hence more continental climates in the eastern parts of these land masses. Similar features can be seen over the southern hemisphere continents too, but these are present to a much lesser extent.

The intra-annual variability of the temperature structure at the 850 mbar level is summarized by the mean calendar monthly distribution of zonal mean values over the 10 year period in Figure 2.5. Here a notable difference between the

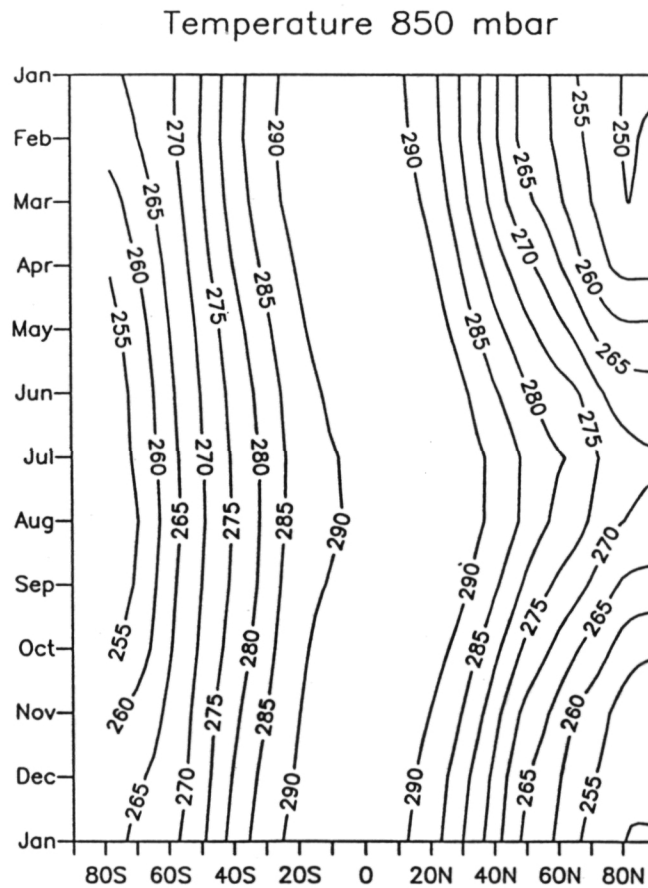


FIGURE 2.5. Mean calendar monthly zonal mean temperature over 1980–1989 at the 850 mbar level, showing intra-annual variability. Units are kelvins.

hemispheres is evident. Whereas a strong annual cycle exists in the northern hemisphere, especially at middle latitudes, a much weaker one occurs in corresponding southern latitudes. For example, the difference between zonal mean temperatures in the extreme months of January and July is 20 °C near 40° N but only 7 °C near 40° S. Such a difference is due to the contrasting land–ocean distributions of the hemispheres. As was evident in Figure 2.4, the highest temperatures occur near 10° N and are highest for the year during July and August; corresponding temperatures during January and February are not quite as warm near 10° S.

The anomalies from the mean temperature at each latitude over the 10 year period are reasonably small (figure not shown). The zonal mean temperatures do not vary in any year and at any latitude by more than 2 °C, fluctuating weakly during the period. However, the period around 1986–87 is colder than the rest of the decade, particularly in the middle latitudes of the northern hemisphere, but it is warmer again at the end of the decade 1988–1989.

2.4.3 Wind Structure

The zonal mean zonal wind for the 10 year period, given in Figure 2.6, shows a relatively symmetric structure in both hemispheres, with westerly winds

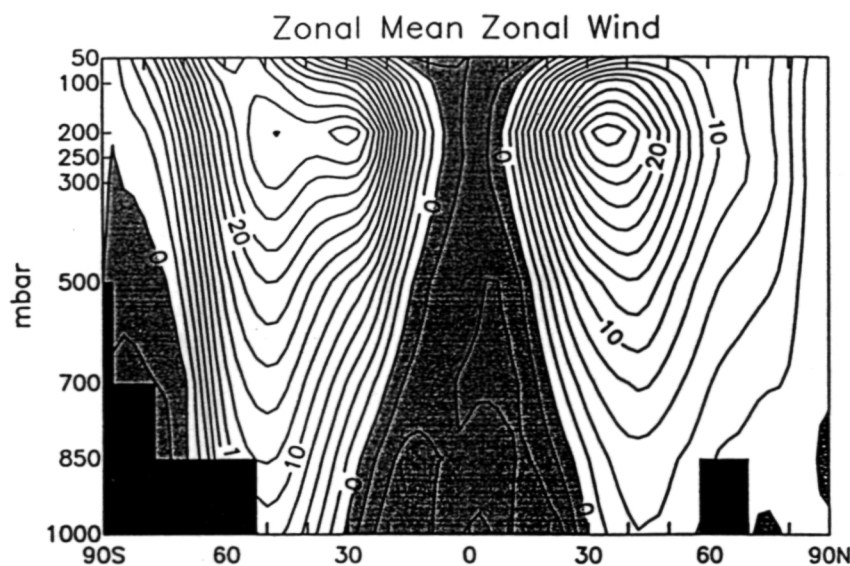


FIGURE 2.6. Zonal mean zonal wind for 1980–1989 between the 1000 and 50 mbar levels. Units are m s^{-1} . Positive values indicate westerly winds, negative values easterly winds; winds are shaded.

predominating throughout much of the globe. However, easterly winds do occur in the lowest latitudes, especially in the lower levels. Indeed, at the surface, easterly winds are observed between 30° N and S, spanning half the area of the globe. Weak easterlies also occur to some extent in the lower altitudes of the polar regions.

Typically the winds become more westerly as they increase with height up to around 200 mb. In this way, in the lower latitudes, winds change from an easterly to a westerly direction and in the middle latitudes, strong westerly jets occur. The major jets have their strongest mean near the 200 mbar level. The annual mean values of the jet maxima reach 27 and 29 m s^{-1} in the northern and southern hemispheres, respectively. This overall increase in winds with altitude is connected by the geostrophic relationship to the meridional temperature gradient. The somewhat stronger winds in the southern hemisphere are consistent with the larger such gradient in that hemisphere.

The mean zonal winds at the 200 mbar level during the decade are given in Figure 2.7. This figure shows the general restriction of the easterlies at this level to the deep tropics in a band with one portion extending from western Africa to the western Pacific, maximizing across the "maritime continent" of Indonesia. Also, there is a smaller portion of easterlies extending westward from South America. The central core of the easterly winds, with values exceeding 10 m s^{-1} , is over Indonesia, a region of intense heating and convection. In general, the wind becomes less easterly and switches to westerly (more positive) the more poleward one goes in latitude. Large values occur off the storm track regions to

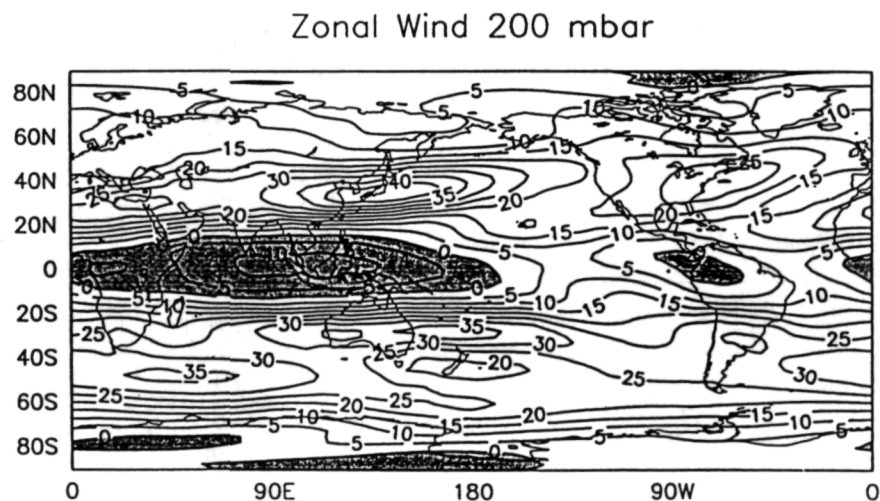


FIGURE 2.7 Mean zonal wind for 1980–1989 at the 200 mbar level. Units are m s^{-1} .

the east of the major northern continents, especially off Japan, where the wind magnitude exceeds 40 m s^{-1} , and off North America. Of particular prominence also are the zonal winds in a band across the middle southern latitudes, maximizing over the southern Indian Ocean.

The seasonal variations in the zonal winds are considerable, as is seen in Figure 2.8, which gives their progression during the calendar year at 200 mbar. Mean easterlies in the tropical band are strongest during July and August, exceeding 10 m s^{-1} ; these disappear by December. A strong meridional gradient of wind occurs between tropics and subtropics, especially during the winter months of the respective hemisphere. The amplitude of the annual signal in mean

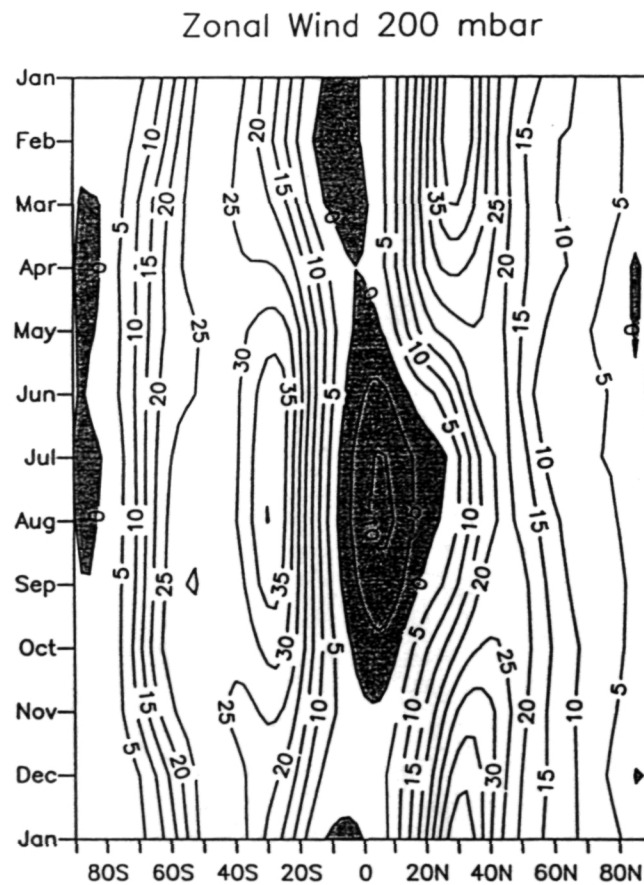


FIGURE 2.8. Mean calendar monthly zonal mean zonal wind over 1980–1989 at the 200 mbar level, showing intra-annual variability. Units are m s^{-1} .

zonal wind, strongest in the subtropics, is exceeded in the southern hemisphere by its value in the northern one. Indeed, for this reason, the seasonal signature of the global mean angular momentum of the atmosphere is that of the northern hemisphere (Rosen and Salstein, 1983). The strongest mean value of the zonal jet, at 30° N, exceeds 40 m s^{-1} in January. Interannual variability during the decade is demonstrated by the anomalies in Figure 2.9, which are strongest in the northern subtropics. Of note are the maxima in 1983 and 1987, years during which major ENSO events occurred; in these two years, winds were particularly strong across the subtropics, especially over the Pacific, consistent with analyses of ENSO behavior.

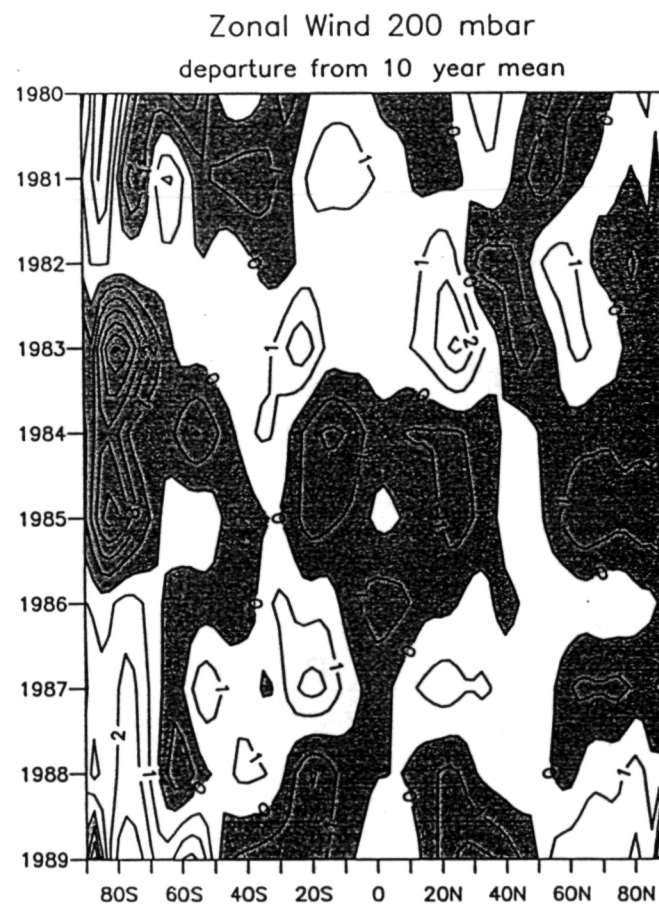


FIGURE 2.9. Mean annual zonal mean zonal wind anomalies over 1980–1989 at the 200 mbar level, showing interannual variability. Units are m s^{-1} .

The mean meridional wind structure and the mean vertical motions are tied together over long periods through the conservation of mass relation, as noted in Section 2.2. From equation (2.1) a picture of the mean meridional circulation can be formulated in terms of a mass streamfunction, given for the 10 year period, in Figure 2.10. In the figure, the mean flow follows the streamfunction isolines, which are given in units of $10^{10} \text{ kg s}^{-1}$. Furthermore, the strength of the flow is proportional to the cross-isoline gradient. The figure reveals a multicell pattern for the meridional circulation in the atmosphere, which in the tropics contains a direct (Hadley) cell in each hemisphere. The areas of upward motion in these Hadley cells extend between 20°N and 10°S , and the related downward flow occurs in the subtropics between 20° and 40°S and between 20° and 40°N . Because the rising branches are relatively warmer than the sinking ones, the net result is considered a thermally direct circulation. The southern Hadley circulation is stronger than the northern one in this annual mean picture. Because of the mass continuity principle, there is low-level equatorward motion in the low-latitude areas of the Hadley cells and corresponding poleward motion in the upper atmosphere. The centers of the cells are near the 700 mbar level in this analysis, but they have been somewhat higher in analyses based on rawinsonde data alone (Peixoto and Oort, 1992). Poleward of the Hadley cells are the

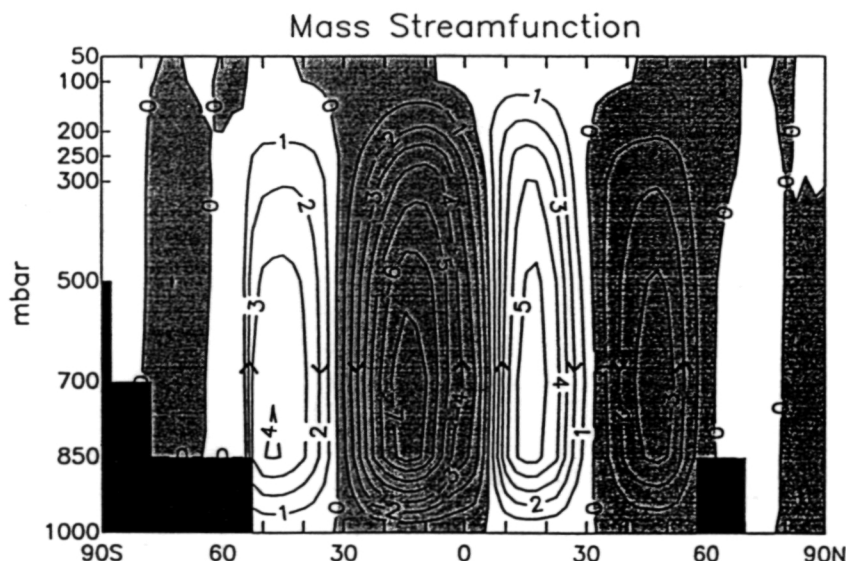


FIGURE 2.10. Cross-section of the mass streamfunction for the mean meridional circulation for 1980–1989 between the 1000 and 50 mbar levels. Units are $10^{10} \text{ kg s}^{-1}$. Positive values indicate clockwise circulation.

"indirect" Ferrel cells, which have rising motion in their lower-latitude sections, and hence in warmer conditions, than where sinking motion occurs. The meridional motions of the Ferrel cells are reversed from those of the tropical Hadley cells and in fact are driven by different dynamical processes than are the Hadley cells, mostly by synoptic-scale eddies. Lastly, there are weaker direct cells poleward of the Ferrel cells, with corresponding meridional flow aloft.

The meridional circulations for the two individual solstitial seasons, however, are very different from this annual mean picture, as can be seen in Peixoto and Oort (1992). Indeed, the annual mean meridional circulation in Figure 2.10 appears to be a combination of quite different values from all parts of the year. When looking at streamfunctions representing a single season, the twin Hadley circulation reduces to a strong one in the winter hemisphere and a much weaker one in the summer hemisphere. Furthermore, the stronger Hadley cell is displaced meridionally toward the summer hemisphere, following the motion of the sun with the seasons. The Ferrel cells are slightly increased in their respective winter hemispheres, too. Of course the mean meridional winds also follow the flow at upper and lower levels in the latitudes of the Ferrel cell. Fluctuations in the winds within meridional zones tend to be organized with alternations of sign, consistent with zonal wavenumber signals around a hemisphere of up to 6.

2.4.4. Humidity Structure

Water vapor is distributed throughout the lower troposphere and is a rather variable and mobile atmospheric constituent. A number of different parameters may be used to represent humidity: these include mixing ratio, the proportion of water vapor to dry air by mass, specific humidity, the proportion of water vapor to total air, and relative humidity, the fraction of specific humidity to the maximum specific humidity possible for a given temperature and pressure, as determined by a comparison with the saturation vapor pressure. Specific humidity is often the quantity considered for purposes of assessing the role of water vapor in overall water budgets. To a large extent, humidity patterns are similar to those of temperature but are also related to atmospheric pressure level because of the dependence of saturation vapor pressure on these two parameters. Specific humidity varies, though, according to air mass characteristic as well.

The basic pattern of zonal mean specific humidity, given in Figure 2.11, shows a maximum at the 1000 mbar level of 19 g kg^{-1} , equivalent to a proportion of nearly 0.2% of atmospheric mass. This value decreases with altitude to 2 g kg^{-1} by the 500 mbar level in the tropics. Also, at the 1000 mbar level, specific humidity decreases with temperature, and hence latitude, to 2 g kg^{-1} by about 65°S and 75°N . The zonal mean structure of water vapor is quite similar in the two hemispheres, although the northern hemisphere tends to hold somewhat more water vapor than does the southern one. A map of specific humidity at

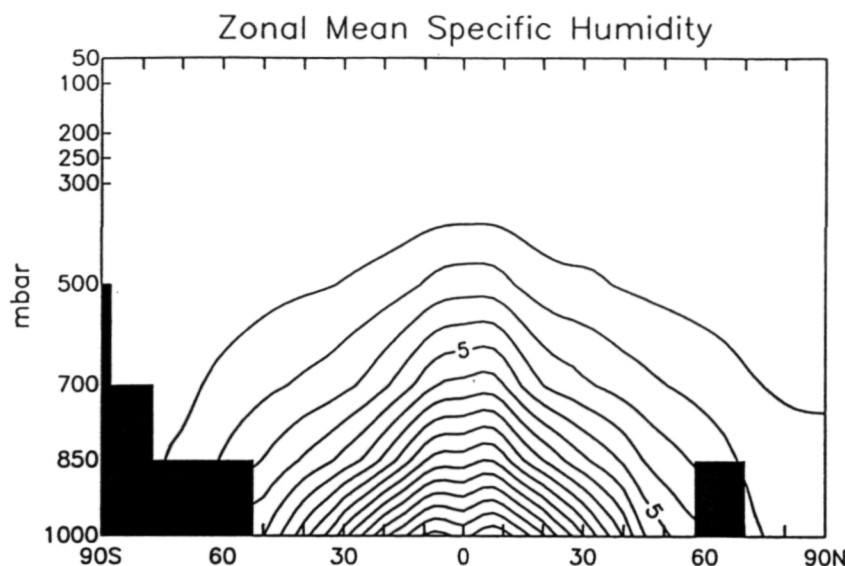


FIGURE 2.11. Zonal mean specific humidity for 1980–1989 between the 1000 and 50 mbar levels. Units are g kg^{-1} . Isolines are spaced every 1 g kg^{-1} .

850 mbars (Figure 2.12) reveals a generally axisymmetric distribution with latitude; however, there is a preference for higher specific humidity over certain regions such as the west tropical Pacific, over Indonesia, and over the Amazon basin. Less moist areas, under 4 g kg^{-1} , exist for central and eastern Asia,

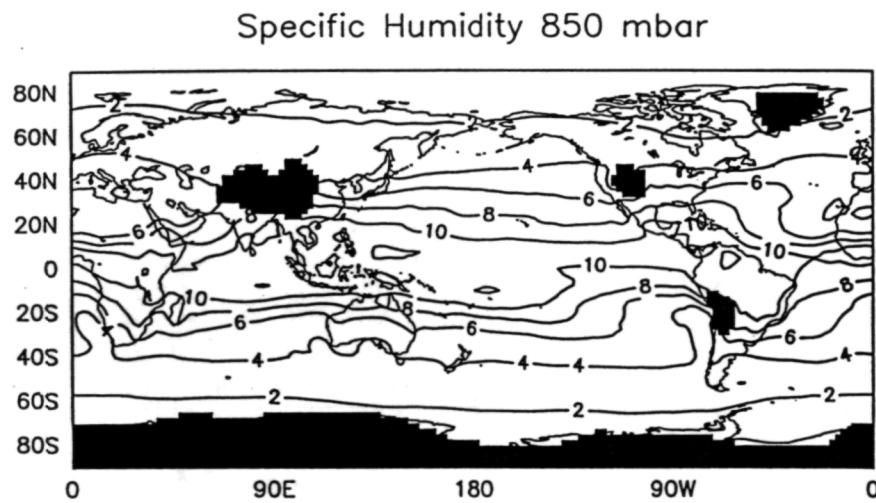


FIGURE 2.12. Mean specific humidity for 1980–1989 at the 850-mbar level. Units are g kg^{-1} .

northern Africa, and western Asia, and these are relatively dry for their latitudes. The annual distribution of water vapor, when given as calendar monthly means, has relatively large and small annual cycles in the southern and northern hemispheres, respectively, with temperate latitudes, varying by as much as 5 g kg^{-1} from maximum to minimum in middle northern latitudes. January and July tend to be the two extreme months for the distribution of water vapor in both hemispheres.

2.4.5 Meridional Eddy Transport of Heat and Momentum

Analyses of atmospheric energy and momentum budgets, especially for zonal mean quantities (Peixoto and Oort, 1992), require that considerable transports of these quantities exist in the meridional direction. These fluxes have been studied intensively, and, as mentioned above, to help understand the dynamics, such transports are often decomposed into their mean and eddy portions. The mean transport of heat, proportional to the average of the product of meridional wind and temperature, is quite consistent with the mean meridional circulation, reviewed in Section 2.4.3. At low levels, heat is transported southward in the northern hemisphere tropics and southern hemisphere middle latitudes, while northward flow of heat occurs in the other portions of the hemispheres near the ground. The transports aloft in the upper troposphere are reverse, completing the signatures of the mean meridional cells.

The zonal mean values of the transient eddy transport of heat for the decade are displayed in Figure 2.13. This transport is poleward nearly everywhere, at both lower and upper levels in both hemispheres. Especially strong values occur poleward of 20° N and S , however. In this way the atmosphere has arranged itself to carry the excess heat absorbed at the low latitudes into the higher latitudes where there is a relative deficit of heating. These eddy transports, proportional to the temporal covariance of the meridional wind and temperature, denoted by $[v' T']$, maximize between 40° and 50° in both hemispheres and at the 850 mbar level.

In a similar fashion the eddy transport of momentum, proportional to the temporal covariance of the meridional and zonal wind ($[v' u']$), is given in Figure 2.14. The distribution of this momentum transport is toward the poles throughout the low to middle latitudes. However, farther poleward in both hemispheres, transport toward lower latitudes occurs. Thus there is an area of convergence of momentum by the transient eddies in middle to high latitudes, between the maxima of opposite signs. In this way the strong jets in these regions are continually maintained against any dissipation that would occur.

In recognition that both the eddy transport of heat and momentum in middle latitudes act to maintain the whole indirect Ferrel cell, a unified view of the

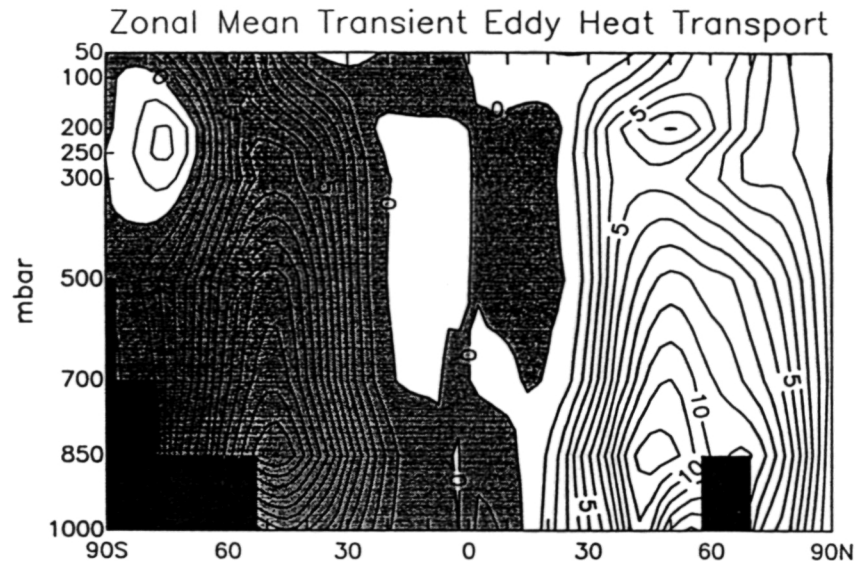


FIGURE 2.13. Zonal mean meridional values of $\sqrt{v'T'}$, proportional to transport by transient eddies of heat, for 1980–1989 between the 1000 and 50 mbar levels. Units are km s^{-1} .

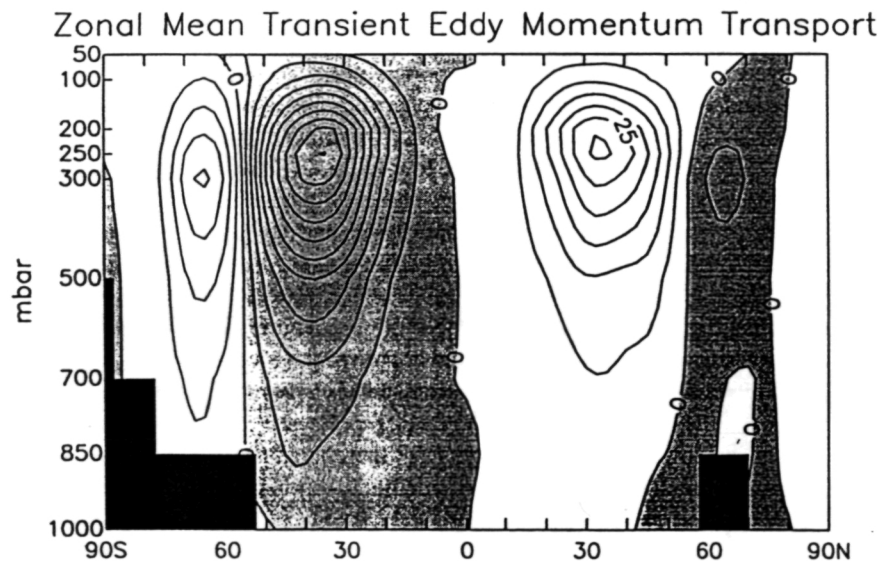


FIGURE 2.14. Zonal mean meridional values of $\sqrt{v'u'}$, proportional to transport by transient eddies of momentum, for 1980–1989 between the 1000 and 50 mbar levels. Units are $\text{km}^2 \text{s}^{-2}$.

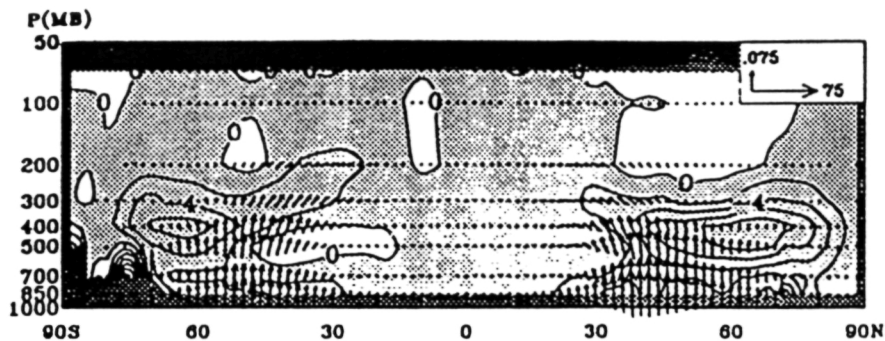


FIGURE 2.15. Meridional cross-section of the transient eddy Eliassen-Palm flux and contours of its divergence, related to the driving of zonal winds by the transient waves, based on seven winters, from meteorological analyses. Horizontal and vertical vector scales (units of 10^7 kg s^{-2}) are displayed in the upper right-hand corner. Contour interval is $2 \text{ m s}^{-1} \text{ day}^{-1}$. (Taken from Black 1993.)

diagnostics of atmospheric wave dynamics has been developed over the last decade. It has as a fundamental invariant quantity, a vector F known as the Eliassen-Palm flux, lying in a meridional plane, whose meridional component F_y and vertical component F_p involve eddy fluxes in the northward direction of angular momentum and heat, respectively (Edmon et al., 1980). Such a flux may be given by

$$\begin{aligned} F_y &= \rho_0 a \cos \phi [\overrightarrow{-v_g u_g}] \\ F_p &= \rho_0 a \cos \phi [\overrightarrow{v_g \theta} \cdot f \theta_p] \end{aligned} \quad (2.5)$$

where v_g and u_g are the meridional and zonal geostrophic wind, respectively, θ is the potential temperature, θ_p is the static stability, ρ is the density, a is the radius of the Earth, and f is the Coriolis parameter. The divergence of F is a measure of the acceleration of the zonal mean zonal wind by wave activity forcing, and so it has zero divergence for wave-like conservative flow. A measure for mean winter conditions of the Eliassen-Palm flux vector and its divergence is given in Figure 2.15. Upward and equatorward fluxes of wave activity occur from the surface at middle latitudes.

2.5. HEATING OF THE ATMOSPHERE

Although the Sun is ultimately the source of energy reaching the Earth, only about 64% of the energy from the radiation intersected by the Earth is actually absorbed in the atmosphere. The remainder is reflected from the surface and from

the clear and cloudy atmosphere. The atmosphere is heated by a number of specific processes, including heating directly by solar radiation, by terrestrial radiation, by sensible processes consisting of conduction and vertical mixing, and by latent processes, which constitute the heat liberated during a change in phase of water substance in the atmosphere.

The radiation consists of short-wave processes, peaking in the visible at wavelength $0.5\text{ }\mu\text{m}$, whose source is the Sun, and long-wave processes, peaking in the infrared near $10\text{ }\mu\text{m}$, whose source is radiation emitted from the Earth. The difference in the frequency of radiation results from the vastly different temperatures of the solar and terrestrial surfaces: the wavelength of maximum emission is inversely proportional to the temperature at which it is emitted (Wien's law). Also, radiation is re-emitted by the atmosphere in the long-wave band, based on its temperature. Solar radiation varies strongly with season and time of day in relation to the elevation angle of the Sun. Heat is absorbed in the atmosphere particularly by water vapor molecules in the lower troposphere, with peaks in the visible and near-infrared spectral regions, and is also strongly transmitted to the atmosphere in the absorption bands in the far infrared. Carbon dioxide also has peaks of absorption in the visible and infrared, while ozone, in particular, greatly absorbs ultraviolet radiation.

Sensible heating involves contact with the ground and transfer of heat between levels within the atmosphere. Near the very lowest level the transport from the ground takes place by means of turbulent exchanges in the boundary layer (Section 2.6). Above that layer, sensible exchanges occur but are not nearly as strong.

Latent processes are often negative, providing cooling, near the lowest layer of the atmosphere where evaporation occurs, but condensation to clouds provides positive heating higher in the free atmosphere. Condensation, and hence cloud formation, occurs by means of a number of distinct processes, including those on large scales and on smaller convective scales.

A summary of the heating processes in terms of the zonal mean average of the four heating components is given in Figures 2.16–2.19 for the area above the lowest part of the boundary layer. These results have been obtained from an annual simulation by the global analysis and forecast model of the NASA Goddard Laboratory for Atmospheres. The latent processes within the model, in particular, are treated in a sophisticated manner, involving complex interactions within detailed cloud convection schemes (Arakawa and Schubert, 1974; Sud and Walker, 1993). The heating rates due to clouds are high over the tropical areas, reaching, for mean annual conditions, as much as 3 K day^{-1} as a result of the strong convective activity (Figure 2.16). This maximum occurs at a rather high level near 400 mbar, revealing the very deep convection in this warm region, reaching into the middle and even the upper troposphere. Maps of latent heating reveal particularly strongly convective areas to include the maritime continent

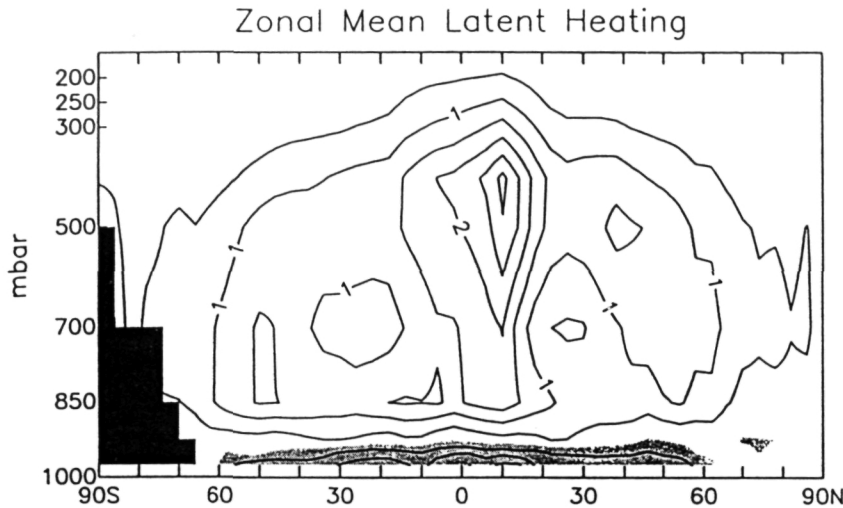


FIGURE 2.16. Zonal mean latent heating for 1 year based on a simulation using the NASA Goddard Laboratory for Atmospheres global circulation model, with physics modified by Sud and Walker (1993). Units are K day^{-1} , with isoline increments of 0.5 K day^{-1} . Negative values are shaded and indicate cooling.

(Indonesia) and South America. Minima of heating occur in the subtropics, in the region of reduced convection near the descending cells. Farther poleward, maxima in the latent heating rate occur again, with the middle-latitude values resulting from shallower convective activity and large-scale cloudiness, though some deeper convection can occur there too. For individual months the maxima are much stronger than the annual average in Figure 2.16, because the maxima are confined to reasonably narrow latitude bands which move with the solar forcing. For example, in July the middle tropospheric maximum in heating reaches over 4 K day^{-1} , centered at 10° N . Nearest the surface, in a shallow area, particularly in the tropics, cooling due to evaporation occurs. Patterns of latent heating are of smaller scale for much shorter time periods. Such latent heating accompanies convective activity and apparently can move horizontally with weather systems.

Sensible heating (Figure 2.17) is strongest at the surface; in the lowest part of the boundary layer (not shown) it is particularly strong, but values are near 1 K day^{-1} by the top of the boundary layer too. Positive values are seen throughout almost the entire globe for annual means of sensible heating owing to the transfer of heat from the relatively warm surface of the Earth below the atmosphere. In particular, ocean surfaces contain much heat, which is evident in maps of mean low level sensible heating, strong over the warm ocean currents. For example, the air over the extension of the Gulf Stream has much sensible

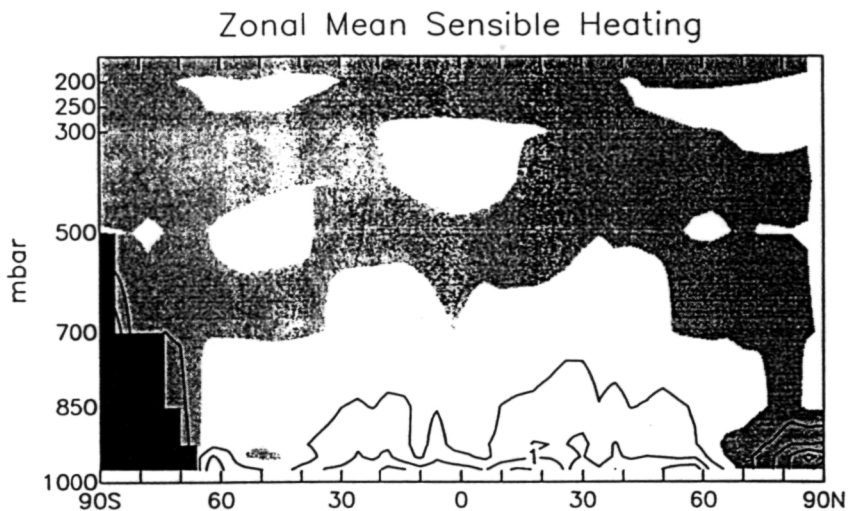


FIGURE 2.17. Same as Figure 2.15, but for sensible heating.

heating evident even north of 70° N, near Scandinavia. However, in the mean, there is some cooling by sensible processes at the lower-boundary near-polar regions because of heat transfer to the cold continents and ice surfaces below. Sensible heating typically decreases with altitude quite quickly, and by the middle troposphere the magnitude of heating decreases to where regions of small positive and negative values are about equal in size. The annual cycle of sensible heating is similarly dependent on factors such as the temperature of the surface.

Annual mean zonally averaged short-wave radiational heating (Figure 2.18) occurs in a symmetric pattern from pole to pole, with the highest values, as expected, at the equator near the surface, exceeding 2 K day^{-1} . However, near the 900 mbar level a fairly constant mean value of short-wave heating, 1 K day^{-1} , occurs at all latitudes. On the other hand, the long-wave processes (Figure 2.19) contribute to cooling throughout the atmosphere, and do so by as much as 2 K day^{-1} over much of the tropics.

As described above, the means of the sensible, latent, and short-wave radiational heating components each increase from equator to poles and are thus positively correlated with the mean temperature pattern. Because of this distribution, their actions tend to increase the existing meridional temperature gradient and, in so doing, increase the potential energy available for the atmosphere to convert to kinetic energy. Conversely, long-wave radiation is negatively correlated with temperature, cooling in relatively warm areas and vice versa. Long-wave radiation thus acts to reduce this potential energy. Never-

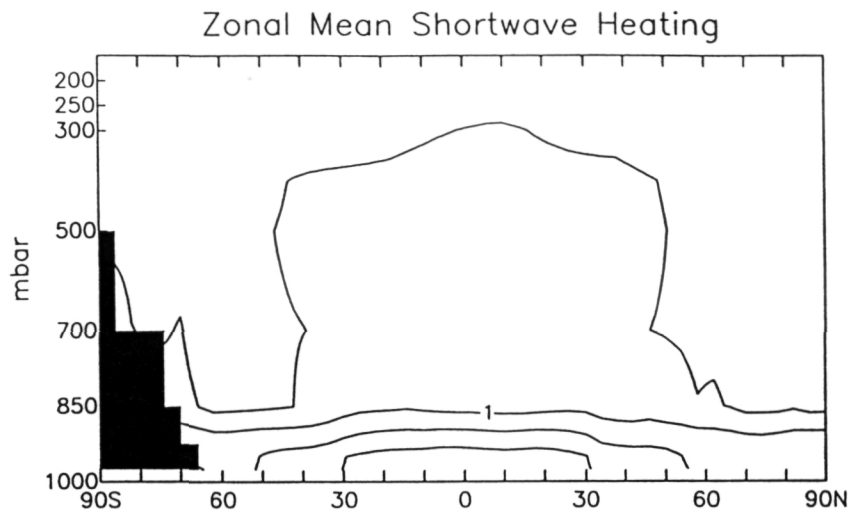


FIGURE 2.18. Same as Figure 2.15, but for short-wave radiational heating.

theless, the reduction due to the long-wave term is less than those of the other three diabatic heating terms, and so, overall, the meridional distribution of heating helps to maintain the energy cycle which is responsible for the general circulation of the atmosphere.

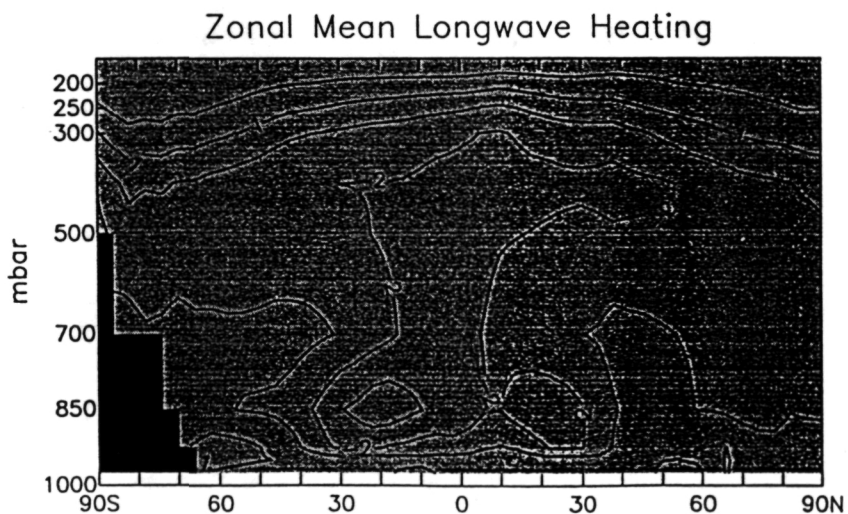


FIGURE 2.19. Same as Figure 2.15, but for long-wave radiational heating.

2.6. BOUNDARY LAYER OVERVIEW

The atmospheric boundary layer has been defined as that portion of the atmosphere nearest the ground having considerable variations over the course of a day; this is in contrast with the free atmosphere above it, whose diurnal fluctuations are more limited. Also, in the boundary layer the major transfer of momentum, heat, and water vapor with the underlying surface occurs, in the first few centimeters, chiefly by molecular diffusion, but above this area, by turbulent diffusion. Although it may vary considerably with region, season, and time of day, the typical height of the boundary layer is 1 km, or about the 900 mbar level.

The structure of the boundary layer in particular is much dependent on its vertical stability, including the type of air mass in which it is embedded. The basic stability is related to the temperature lapse rate of a parcel of air. If virtual potential temperature (the temperature that the air would achieve were it to release its latent heat and be brought to a reference level) increases with height, the air is unstable and convection readily occurs. Conversely, a stable portion of the air mass is one in which an inversion has formed, limiting the upward motions associated with convection. In a dry air mass without cloud cover, ground cooling leads to strongly stable air, hindering convective activity. In a moist cloudy air mass the usual nighttime ground surface cooling may not occur, tending to keep the air in the subcloud layer unstable. Advection of warmer air above a cooler surface layer may create an inversion as well. A simple picture of an inversion layer below the free unstable portion of the troposphere is given in Figure 2.20.

Treatments of the atmospheric boundary layer have divided it into several sublayers whose properties are very dependent on the time of day and typically change with the diurnal cycle (see review by Stull, 1988). Over land surfaces the

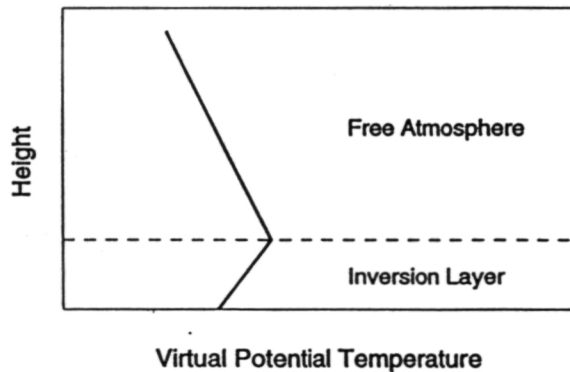


FIGURE 2.20. Schematic of a low inversion layer in which the atmosphere is stable, thus hindering convection.

boundary layer often has a well-defined structure. Above a very shallow surface layer during the daytime is the mixed layer, developing often as a result of convection related to solar heating of the Earth's surface. During the course of the first few hours after sunrise, turbulent exchanges form an even distribution of heat, momentum, and moisture; such can be seen as constant values of virtual potential temperature, wind, and specific humidity. This mixed layer is at a maximum depth in the late part of the afternoon, and, when convection brings air above the level where condensation takes place, clouds form. After sunset, however, the actions of a radiatively cooled ground change the lowest layer into one with a vertically stable distribution. This stable boundary layer grows between sunset and the first hours after dawn, and its turbulent structures are much reduced compared with those of the mixed layer. The portion of the daytime mixed layer that exists into the night-time hours and is located above the stable boundary layer has been termed the residual layer; in this residual layer the concentration of any passive quantities (tracers) that were placed into the atmosphere in the daytime mixed layer remain relatively constant. Convection no longer occurs in this neutrally stratified layer and the turbulence is isotropic. After sunrise on the next day a new mixed layer forms, taking properties, including entrained moisture, from the night-time residual layer and the stable boundary layer underneath.

Transport in the boundary layer of the quantities occurs from areas of high concentrations to those of lower ones, and so vertical eddy fluxes are often modeled by a relationship proportional to the vertical gradient of the respective quantities. For example, the transient eddy flux of heat, F_H , can be given by

$$F_H = \rho c_p \overline{w' T'} \quad (2.6)$$

and parameterized as

$$F_H = -K_H \rho c_p \partial \bar{\theta} / \partial z \quad (2.7)$$

where K_H is the eddy diffusion term for heat, c_p is the specific heat of air at constant pressure, w is the vertical motion, θ is the potential temperature, and ρ is the density. Alternatively, a drag coefficient dependent on conditions in the lowest layer can be determined, so that the flux of heat is related to the local wind velocity and the difference in potential temperature across the very lowest layers of the atmosphere.

2.7. MAJOR EXCHANGES IN THE ATMOSPHERE

The circulation, as viewed in the mean meridional plane, has been reviewed in Section 2.4.3; especially strong in this regard are the tropical Hadley cells, which

transport air between upper and lower levels as well as meridionally. When cross-sections of flow are taken instead in the longitude-height plane, some of the local regions important in vertical transports emerge. One such system has been observed over the Pacific region in low latitudes and has been termed the Walker circulation. The Walker cell typically has rising and descending motions in the eastern and western Pacific areas respectively. However, these motions are variable and their centers move with the annual cycle, related to the predominant convergence zones. Observational evidence exists for strong vertical transport of tropospheric air into the stratosphere, particularly from strong convective activity in the tropics (e.g., Newell and Gould-Stewart, 1981). The very high level of cumulonimbus tops, sometimes to at least 20 km, can be responsible for exchanges of tropospheric and stratospheric air, including deposits of water vapor in the stratosphere (WMO, 1985). In the extratropics, air of tropospheric and stratospheric origins can usually be differentiated by the amounts of potential vorticity P , a quantity defined as

$$P = \alpha \nabla \theta \cdot (\nabla \times V + 2\Omega) \quad (2.8)$$

where $\nabla \theta$ is the gradient of potential temperature and Ω is the angular velocity of the Earth. The absolute vorticity, in parentheses, consists of the curl of velocity plus the vorticity of the Earth's rotation, or twice Ω . For adiabatic and frictionless motion, typical to a large extent in the free atmosphere, the amount of P in a parcel of air is conserved and so the origin of an air mass can often be traced to its value of P . Stratospheric air usually has much larger values of P than does tropospheric air. Gradients in P do arise from mixing of tropospheric and stratospheric air masses from a folding of the tropopause, as suggested by Danielson (1968). In such cases, trace gases and aerosols from the lower stratosphere are mixed into the tropospheric air.

To find the horizontal as well as vertical exchanges within major atmospheric compartments, relatively inactive tracers have been utilized in models. Prather et al. (1987), for example, compared results from a three-dimensional chemical tracer model (CTM) with the observed distribution of quantities of chlorofluorocarbons to study air mass exchanges. The place and time of year of maximum air mass transport have been studied in this manner. For example, interhemispheric exchanges are found to occur mainly in the upper troposphere, and horizontal winds in the summer have been found to be more efficient in carrying tracers away from their sources, while in the winter, vertical transports predominate, elevating concentrations higher in the atmosphere.

Modelers have often treated the average exchanges of mass across the boundaries of the hemispheres and of vertical regions as transfers between four compartments (northern troposphere, northern stratosphere, southern troposphere, and southern stratosphere), modeling such exchanges with coefficients κ

TABLE 2.2 Exchange Times Between Atmospheric Compartments

Exchange	Range (years)	Average (years)
Northern troposphere/Southern troposphere	0.7–1.8	1.0
Stratosphere/Troposphere	0.8–2.0	1.4
Northern stratosphere/Southern stratosphere	3–6	4.0

Source: Adapted from Warneck (1988).

whose inverse τ represents the time constant for decay of the compartment's air content (Warneck, 1988). By taking the observed increase in CO₂, for example, as the slope of their trend, and using an equation for the exchange of air between the compartments, one obtains

$$\frac{d(m_{NT}-m_{ST})}{dt} = -2 \kappa_{NT,ST} (m_{NT}-m_{ST}) + 2R \quad (2.9)$$

where m_{NT} and m_{ST} are the mixing ratios of the tracers in the northern and southern tropospheres respectively, $\kappa_{NT,ST}$ is the exchange coefficient (in year⁻¹) between these regions, and R is the annual CO₂ rise. Equation (2.9) has an exponential solution, for which its variable, the difference in mixing ratios, relaxes to a steady state after a time of the order of $\tau_{NT,ST} = 1/\kappa_{NT,ST}$. Estimates of exchange times using such methods are given in Table 2.2, where a range from different estimates is quoted. In general, northern troposphere/southern troposphere exchanges are the fastest, with many values near $\tau = 1$ year, stratosphere/troposphere exchanges are somewhat slower ($\tau \approx 1.4$ years), and intrastratosphere exchanges are the slowest ($\tau \approx 4$ years).

Acknowledgments

The author wishes to give his sincere thanks to Peter Nelson of AER, Inc., who ably produced most of the figures in the chapter. One figure was taken from a report by R.X. Black of AER, Inc. J. Janowiak of NOAA/NMC assisted with the interpretation of the Climate Diagnostics Data Base. Y. Sud of the NASA Goddard Space Flight Center provided the atmospheric modeling results from which I obtained the diabatic heating measurements. R. Rosen of AER, Inc. has reviewed and helped improve the manuscript. Partial support for the writing of the chapter was under contract NAS5-31333 to AER, Inc. from NASA under its Climate Modeling and Analysis Program.

References

- Arakawa, A. and Schubert, W. H. (1974). Interaction of a cumulus cloud ensemble with the large-scale environment, Part I. *J. Atmos. Sci.*, **31**, 674–701.

- Black, R.X. (1993). Validating seasonal and intraseasonal wave activity in GLA GCM's and data assimilations. *Proc. Seventeenth Ann. Climate Diagnostics Workshop*, US Department of Commerce, NOAA/NWS/CAC/NMC, pp. 236–237.
- Danielson E.F. (1968). Stratospheric-tropospheric exchange based on radioactivity, ozone, and potential vorticity. *J. Atmos. Sci.*, **25**, 502–518.
- Edmon, H.J., Hoskins, B.J. and McIntyre, M.E. (1980). Eliassen-Palm cross sections for the troposphere. *J. Atmos. Sci.*, **37**, 2600–2616.
- Johnson, D. (1989). The forcing and maintenance of global monsoonal circulations: an isentropic analysis. In Saltzman, B., Ed., *Advances in Geophysics*, Academic Press, New York, NY, pp. 43–316.
- Kalnay, E. and Jenne, R. (1991). Summary of the NMC/NCAR reanalysis workshop of April 1991. *Bull. Am. Meteorol. Soc.*, **72**, 1897–1904.
- Kanamitsu, M. (1989). Description of the NMC global data assimilation and forecast system. *Weather Forecast.*, **4**, 335–342.
- Madden, R. and Julian, P.R. (1971). Detection of a 40–50 day oscillation in the zonal wind in the tropical Pacific. *J. Atmos. Sci.*, **28**, 702–708.
- Newell, R.E. and Gould-Stewart, S. (1981). A stratospheric fountain? *J. Atmos. Sci.*, **38**, 2789–2796.
- Oort, A.H. (1983). Global atmospheric circulation statistics, 1958–1973. *NOAA Professional Paper 14*, US Government Printing Office, Washington, DC..
- Peixoto, J. P. and Oort, A.H. (1974). The annual distribution of atmospheric energy on a planetary scale. *J. Geophys. Res.*, **79**, 2149–2159.
- Peixoto, J.P. and Oort, A.H. (1992). *Physics of Climate*, American Institute of Physics, New York, NY.
- Philander, S.G.H. (1989). *El Niño, La Niña and the Southern Oscillation*. Academic Press, New York, NY.
- Prather, M., McElroy, M., Wofsy, S., Russell, G. and Rind, D. (1987). Chemistry of the global troposphere: fluorocarbons as tracers of air motion. *J. Geophys. Res.*, **92**, 6579–6613.
- Rasmusson, E.M. and Arkin, P.A. (1985). Interannual climate variability associated with the El Niño/Southern Oscillation. In *Coupled Ocean Atmosphere Models*, Elsevier, Amsterdam, pp. 697–725.
- Rosen, R.D. and Salstein, D.A. (1983) Variations in atmospheric angular momentum on global and regional scales, and the length of day. *J. Geophys. Res.*, **88**, 5451–5470.
- Rosen, R.D., Salstein, D.A., Peixoto, J.P., Oort, A.H. and Lau, N.-C. (1985). Circulation statistics derived from level III-b and station-based analyses during FGGE. *Mon. Weather Rev.*, **113**, 65–88.
- Stull, R. (1988). *An introduction to Boundary Layer Meteorology*, Kluwer Academic Publishers, Dordrecht.
- Sud, Y. and Walker, G. (1993). A rain evaporation and downdraft parameterization to complement a cumulus-updraft scheme and its evaluation using GATE data. *Mon. Weather Rev.*, **111**, 3019–3039.
- Trenberth, K.E. and Olson, J.G. (1988). An evaluation and intercomparison of global analyses from the National Meteorological Center and the European Centre for Medium Range Weather Forecasts. *Bull. Am. Meteorol. Soc.*, **69**, 1047–1057.
- Trenberth, K.E. and Guillemot, C.J. (1994). The total mass of the atmosphere. *J. Geophys.*

- Res.*, 99, 23079–23088.
US Standard Atmosphere (1976). National Oceanic and Atmospheric Administration.
Warneck, P. (1988). *Chemistry of the Natural Atmosphere*, Academic Press, San Diego,
CA.
WMO (World Meteorological Organization) (1985). *Atmospheric Ozone, Report No. 16*,
Geneva.